OPTIMIZATION OF THERMAL LAYOUT DESIGN OF ELECTRONIC EQUIPMENTS ON THE PRINTED CIRCUIT BOARD

Dr. Ihsan Y. Hussain
Mech. Eng. Dept
College of Engineering
University of Baghdad

Hayder Shakir Abdulla
Ph.D. Student
Mech.Eng.Dept
University of Baghdad

ABSTRACT

A thermal layout modeling and optimization routine for a Printed Circuit Board (PCB) has been made in the present work. The thermal model includes the modeling of electronic components based on thermal resistances and the PCB as a flat plate with multiple heat sources. Isothermal and Isoflux natural convection heat transfer for horizontal and vertical PCB thermal modeling. The numerical solution method for the 2-dimensional thermal model is the superposition method for the adiabatic PCB edges. The optimization meshing model was constructed based on the Complex Method. The numerical Complex Method has been improved to a new optimization method named as "Dual Complex Method", which minimize the objective function to give the optimal step sizes in X and Y -directions. The optimization thermal layout model was constructed to accommodate the numerical SUMT mathematical optimization method. Optimization results show that in free convection, and for the optimum total heat loss objective function, the larger dimension of the PCB must be oriented horizontally rather than vertically, and the electronic components or sub-assemblies of large power should be placed near the top of the PCB. In the case of horizontal upset-down in natural convection, the components of large power must be placed near the center of the PCB.

الخلاصه

يتناول البحث الحالي تصميم التوزيع الحراري و الأمثليه لتوزيع المعدات الإلكترونية على اللوحة الإلكترونية. النموذج الحراري للأجزاء الإلكترونية يعتمد على المقاومات الحرارية و الموديل المكعبي، اما اللوحة الإلكترونية المطبوعة تم معاملتها على أساس الصفيحة المستوية مع العديد من المصادر الحرارية. وهذه الموديلات تم إنشائها لانتقال الحرارة بالحمل عند حالتي ثبوت درجة الحرارة والفيض الحراري للوحة الإلكترونية العمودية و الأفقية. تم حل معادلة التوازن الحراري بطريقة الحلول المتكررة"Superposition" لموديل ثنائي البعد مع عزل حافات اللوحة الإلكترونية حراريا. أن النموذج المتضمن أمثلة التقسيم الشبكي(mesh) تم إنشاءها باستخدام الطريقة المركبة Complex Method وهذه الطريقة تم تطويرها للحصول على طريقة مركبة جديدة تسمى الطريقة المركبة الثنائية Dual Complex بحيث يتم تقليل دالة الهدف Objective Function للحصول على قيم خطوات التقسيم step sizes في نظام ثنائي البعد. أن طريقة أمثلة التوزيع الحراري للدوائر الإلكترونية تم إنشائها لتلائم طريقة الأمثلة الرياضية SUMT . نتائج الأمثليه أثبتت بأن البعد الأكبر للوحة الإلكترونية المطبوعة يجب أن يوجه أفقيا" والبعد الآخر عموديا" في حالة الفقدان الحراري الأمثل في الحمل الحر. كذلك فأن الأجزاء الإلكترونية ذات القدرة العالية يجب أن توضع قريبة من قمة

اللوحة الإلكترونية في حالة أمثلة الفقدان الحراري الأمثل في حالة الحمل الحر بالإضافة للوضع العمودي. أما في حالة اللوحة الإلكترونية الأفقية المقلوبة فأن أمثلة انتقال الحرارة تحتم وضع الأجزاء الإلكترونية ذات القدرة العالية قريبة" من مركز اللوحة.

KEYWORDS:Thermal Layout, Design, Electronic Equipments, Printed Circuit Board, Optimization

INTRODUCTION

Increasing clock frequencies on integrated circuits, together with continuous miniaturization, is resulting in widely increased heat dissipation per unit area on PCB. Within avionics, high demands are set regarding optimization of space and weight of devices. At the same time, reliability and functionality requirements are of vital importance.

Lee et. al. (1989) developed a quasi-analytical conjugate heat transfer model for two-dimensional vertical flat plates with discrete heat sources of arbitrary size and power level under natural convection. The plate is located in an extensive, quiescent fluid, which is maintained at uniform temperature. The model consists of an approximate analytical boundary layer solution and a one-dimensional numerical conduction analysis, which on allowance is made to account for radiation heat transfer. **Lee et al. (1990)** developed a conjugate model for airflow over flat plates with arbitrarily located heat sources based on the integral formulation of the boundary layer equations combined with finite volume solution, which assumes two-dimensional heat flow within the plate. The fluid and solid solutions are coupled through an iterative procedure, allowing a unique temperature profile to be obtained at fluid-solid interface. Radiation heat loss is also included in the plate heat transfer **Mahaney et al. (1990)** investigated mixed convection heat transfer from a four-row, in-line array of 12 square heat sources that are flush mounted to the lower wall of a horizontal, rectangular channel. The experimental data encompass heat transfer regimes characterized by pure natural convection, mixed convection, and laminar forced convection, where water was used as a coolant. **Lee et. al.(1991)** examine some of common design of microelectronic circuitry such as the thermal conductivity and surface emissivity of the circuit board under forced convection. The flow velocity of the cooling fluid and positioning and power dissipation on the heat sources, to determine the relative merits of each as means of controlling circuit **Lee et. al. (1991A)** found the parameters on which the operating temperature depends in natural convection heat transfer and they showed the effect of these parameters such as the thermophysical properties, package location, and the applied power level have on localized temperature and average Nusselt number. Also they discussed a specific example of a circuit board and heat source combination. **Lee et al. (1992)** obtained thermal resistance characterization of typical microelectronic packages in terms of an optimization factor, which can provide a useful standard for design and modeling package performance. The various heat flow paths from typical model are outlined, and a variety of package types are modeled, including single-chip and multi-chip package. **Elias and Sridhar (1995)** examined the problem of natural convection of air in horizontal, enclosed air layers, due to localized heating from below. The problem is of great relevance to several electronic cooling applications. The results obtained can help the electronic packaging designer in determining whether heat transfer will be dominated by conduction or convection, for a given module heat dissipation and size of the air gap around the module. **Gerald (2001)** used a superposition method and the adiabatic heat transfer coefficient is introduced. A specific, and highly simplified problem, is considered in detail: the heat transfer from three, uniformly spaced, geometrical identical blocks. The researcher explained how the adiabatic heat transfer coefficient and superposition Kernel function could be measured. A typical piece of electronic equipment has several components mounted on one or more printed circuit boards. **Ying et al. (2002)** optimize the thermal performance of the Integrated Power Electronic Modules IPEM. Three-dimensional active IPEM was modeled using the thermal-fluid analysis program ESC in I-DEAS to study the thermal performance of IPEM. Several design variables including the ceramic material, the ceramic thickness, and the thickness of the heat spreader were modeled to optimize IPEM geometric design and to improve the thermal performance while reduce the footprint.

In the previous works, the authors attempt to solve the energy, continuity, and momentum equation with specified boundary conditions and validated the results by using experimental work. In other words, their results are founded as charts or graphs; therefore, these charts can be translated as equations to the specified cases. In the present work, these equations can be coupled to the optimization program to optimize the thermal design of electronic equipment cooling (passive and/or active cooling). The present work represents a complementary solution for the optimum thermal design.

THERMAL MODEL

The main modeling assumptions are as follows:

1. The temperature distribution $T(X,Y)$ within the board $L_1 \times L_2$ of k_b conductivity and the thickness t_s in two dimension;
2. The convective heat transfer on the upper and lower board faces are characterized by a unique pair (T_∞ , h) where fluid temperature T_∞ and heat transfer coefficient h are uniform;
3. Components are modeled by rectangular heat sources with uniform power Q_i
4. Steady state only is considered.

The boundary conditions along the edges of the PCB, considered to be adiabatic (Lee et. al., 1991A), Then governing equation can be derived as follows(see **Fig. 1a**):

$$\frac{\partial q_x}{\partial X} dX + \frac{\partial q_y}{\partial Y} dY - (q_{conv} + q_{rad}) + \dot{q}\, dXdYt_s \delta = 0 \qquad (1)$$

Where; $\delta = 1$ inside the heat source;

$\delta = 0$ in other PCB regions;

$$q_x = -k_b t_s \frac{\partial T}{\partial X} dY \quad , \quad q_y = -k_b t_s \frac{\partial T}{\partial Y} dX \, ;$$

$$q_{\text{cov}} = hdXdY(T - T_\infty) \quad , \quad q_{\text{cov}} = h_r dXdY(T - T_\infty) \text{; and } q = \frac{Q}{b_i w_i t_s} .$$

Rearranging Eq. (1) yields

$$-(\frac{\partial^2 T}{\partial X^2} + \frac{\partial^2 T}{\partial Y^2}) + \eta^2 (T - T_\infty) = \frac{Q\delta}{k_b b_i w_i t_s} \qquad (1a)$$

The boundary conditions are:

$$\frac{\partial T(0,Y)}{\partial X} = \frac{\partial T(L_1,Y)}{\partial X} = \frac{\partial T(X,0)}{\partial Y} = \frac{\partial T(X,L_2)}{\partial Y} = 0 \qquad (2)$$

With $\eta^2 = \dfrac{(h + h_r)}{k_b t_s}$ (3)

The board temperature is then given by an expansion of the form:

$$T(X,Y) = \sum_{i=0}^{N_x} \sum_{j=0}^{N_y} a_{ij} \cos(\frac{i\pi X}{L_1}) \cos(\frac{j\pi Y}{L_2}) \quad (4)$$

The superposition principle allows computing the board thermal map, i.e. the map of the board equipped with its components, as the sum of the board map assumed to be free of components and of each component thermal map. Accordingly, when a component placement is modified, the operation cycle is as follow:

1- The individual component map is subtracted from the global map;
2- The component map is computed at the new location;
3- This new map is added to the global map.

From computational viewpoint, the second sequence is obviously the critical one.The direct formulation **(Le Jannou and Houn, 1991)** is actually inadequate for an interactive updating of the thermal maps. The algorithm of optimization, through a modified formulation and a careful implementation, whose details are beyond the scope of this article, is the main difficulty in meeting the “real time” requirement. By contrast, seen from the user viewpoint, two parameters are sufficient to control the algorithm numerical behavior. One is used to specify the computational grid density while the other allows control of the accuracy of the series convergence.

Setting the problem also requires the specification of the heat transfer coefficients on the board faces. Providing an assessing tool here circumvents this constant difficulty of thermal simulations. The user interface of this tool allows the designer to characterize rapidly the board cooling configuration: natural convection on a horizontal or vertical board, parallel or impingement flow on a board cooled by forced convection and fluid temperature. Internally, the program uses the physical properties of air and common correlations between the relevant non-dimensional numbers to derive and proposed heat transfer coefficient values. The user remains free to impose his own values.

The air gap R_{gap} thermal resistance is calculated from the following equation:

$$R_{gap} = \frac{\delta_{gap}}{kA_6} \quad (5)$$

Where, A_6 is the area of the lower surface of the electronic component. The junction to board thermal resistance R_{jb} is calculated from the following equation:

$$R_{jb} = R_{jc} + R_{gap} + \frac{l_p}{N_p k_p A_p} \quad (6)$$

Where, N_p, k_p, A_p, and l_p are the number, thermal conductivity, cross-sectional area, and length of the lead pins.

The coefficient of **Eq. (4)** can be calculated by applying it into **Eq. (1a)** at each point in the PCB meshing $(n \times m)$. The electronic component regions can be limited in the expression below:

$(CX_i + b_i / 2, CX_i - b_i / 2, CY_i + w_i / 2, CY_i - w_i / 2)$.

In the present study, the Biot number $(Bi = ht_s / k_b)$ is less than 0.1, and then the temperature difference across the thickness of the board is small and can be neglected. Applying **Eq. (4)** at each point yields:

$$\sum_{i=1}^{N_x}\sum_{j=1}^{N_y} a_{ij}\left(\frac{i\pi}{L_1}\right)^2 \cos\left(\frac{j\pi Y}{L_2}\right)\cos\left(\frac{i\pi X}{L_1}\right) + \sum_{i=1}^{n}\sum_{j=1}^{m} a_{ij}\left(\frac{j\pi}{L_2}\right)^2 \cos\left(\frac{i\pi X}{L_1}\right)\cos\left(\frac{j\pi Y}{L_2}\right) +$$
$$+\eta_{ij}^2 \sum_{i=1}^{N_x}\sum_{j=1}^{N_y} a_{ij}\cos\left(\frac{i\pi X}{L_1}\right)\cos\left(\frac{j\pi Y}{L_2}\right) = \eta_{ij}^2 T_\infty + \frac{q_{ij}}{k_{ij}} \qquad (7)$$

Where, $k_{ij} = k_b$, $\eta_{ij}^2 = \dfrac{h_{ij}}{k_{ij} t_s}$, and $q_{ij=0}$ at the regions that free of modules. Also $k_{ij} = k_e$, and $q_{ij} = Q_{ij} / w_i b_i t_s$ at the element (module). Expanding **Eq. (7)** for 2×2 mesh points (for example) yields:

$$a_{11}\left(\frac{\pi}{L_1}\right)^2 \cos\left(\frac{\pi X_1}{L_1}\right)\cos\left(\frac{\pi Y_1}{L_2}\right) + a_{12}\left(\frac{\pi}{L_1}\right)^2 \cos\left(\frac{\pi X_1}{L_1}\right)\cos\left(\frac{2\pi Y_2}{L_2}\right)$$
$$+ a_{21}\left(\frac{2\pi}{L_1}\right)^2 \cos\left(\frac{2\pi X_2}{L_1}\right)\cos\left(\frac{\pi Y_1}{L_2}\right) + a_{22}\left(\frac{2\pi}{L_1}\right)^2 \cos\left(\frac{2\pi X_2}{L_1}\right)\cos\left(\frac{2\pi Y_2}{L_2}\right)$$
$$+ a_{11}\left(\frac{\pi}{L_2}\right)^2 \cos\left(\frac{\pi X_1}{L_1}\right)\cos\left(\frac{\pi Y_1}{L_2}\right) + a_{12}\left(\frac{2\pi}{L_2}\right)^2 \cos\left(\frac{\pi X_1}{L_1}\right)\cos\left(\frac{2\pi Y_2}{L_2}\right)$$
$$+ a_{21}\left(\frac{\pi}{L_2}\right)^2 \cos\left(\frac{2\pi X_2}{L_1}\right)\cos\left(\frac{\pi Y_1}{L_2}\right) + a_{22}\left(\frac{2\pi}{L_1}\right)^2 \cos\left(\frac{2\pi X_2}{L_1}\right)\cos\left(\frac{2\pi Y_2}{L_2}\right)$$
$$+ \eta_{11}^2 \begin{bmatrix} a_{11}\cos\left(\frac{\pi X_1}{L_1}\right)\cos\left(\frac{\pi Y_1}{L_2}\right) + a_{12}\left(\frac{\pi}{L_1}\right)^2 \cos\left(\frac{\pi X_1}{L_1}\right)\cos\left(\frac{2\pi Y_2}{L_2}\right) \\ a_{21}\cos\left(\frac{2\pi X_2}{L_1}\right)\cos\left(\frac{\pi Y_1}{L_2}\right) + a_{22}\cos\left(\frac{2\pi X_2}{L_1}\right)\cos\left(\frac{2\pi Y_2}{L_2}\right) \end{bmatrix}$$
$$= \eta_{11}^2 T_\infty + \frac{q_{11}}{k_{11}} \qquad (8)$$

The above equation is for the point (1,1). If we define:

$$C_{ij}^{pl} = \left(\left(\frac{i\pi}{L_1}\right)^2 + \left(\frac{j\pi}{L_2}\right)^2 + \frac{h_{pl}}{k_{pl} t_s}\right)\cos\left(\frac{i\pi X_i}{L_1}\right)\cos\left(\frac{j\pi Y_i}{L_2}\right) \qquad (9)$$

$$D_{ij} = \frac{h_{ij}}{k_{ij} t_s} T_\infty + \frac{q_{ij}}{k_{ij}} \qquad (10)$$

Then for the above example, **Eq. (7)** becomes:

$$\begin{bmatrix} C_{11}^{11} & C_{12}^{11} & C_{21}^{11} & C_{22}^{11} \\ C_{11}^{12} & C_{12}^{12} & C_{21}^{12} & C_{22}^{12} \\ C_{11}^{21} & C_{12}^{21} & C_{21}^{21} & C_{22}^{21} \\ C_{11}^{22} & C_{12}^{22} & C_{21}^{22} & C_{22}^{22} \end{bmatrix} \begin{bmatrix} a_{11} \\ a_{12} \\ a_{21} \\ a_{22} \end{bmatrix} = \begin{bmatrix} D_{11} \\ D_{12} \\ D_{21} \\ D_{22} \end{bmatrix} \tag{11}$$

In general for ($n \times m$)mesh points,

$$\begin{bmatrix} C_{11}^{11} & C_{12}^{11} & \cdots & C_{1m}^{11} & C_{n1}^{11} & \cdot\ \cdot & C_{nm}^{11} \\ C_{11}^{12} & C_{12}^{12} & \cdots & C_{1m}^{12} & C_{n1}^{12} & \cdot\ \cdot & C_{nm}^{12} \\ C_{11}^{13} & C_{12}^{13} & \cdots & C_{1m}^{13} & C_{n1}^{13} & \cdot\ \cdot & C_{nm}^{13} \\ \cdot & \cdot & \cdot & \cdot & \cdot & \cdot\ \cdot & \cdot \\ \cdot & \cdot & \cdot & \cdot & \cdot & \cdot\ \cdot & \cdot \\ \cdot & \cdot & \cdot & \cdot & \cdot & \cdot\ \cdot & \cdot \\ C_{11}^{n,m-1} & C_{12}^{n,m-1} & \cdots & C_{1m}^{n,m-1} & C_{n1}^{n,m-1} & \cdot\ \cdot & C_{nm}^{n,m-1} \\ C_{11}^{nm} & C_{12}^{nm} & \cdots & C_{1m}^{nm} & C_{n1}^{nm} & \cdot\ \cdot & C_{nm}^{nm} \end{bmatrix} \begin{bmatrix} a_{11} \\ a_{12} \\ \cdot \\ \cdot \\ a_{1m} \\ a_{n1} \\ \cdot \\ a_{nm} \end{bmatrix} = \begin{bmatrix} D_{11} \\ D_{12} \\ \cdot \\ \cdot \\ D_{1m} \\ D_{n1} \\ \cdot \\ D_{nm} \end{bmatrix}$$

(12)

The above system represents a linear system of $(n \times m) \times (n \times m)$ unknowns with $(n \times m) \times (n \times m)$ equations, which can be solved by Gaussian Elimination Method. The final solution gives the coefficients of **Eq. (4)** that leads to find the temperature distribution $T(X,Y)$ for the complete electronic system cooling.

The temperature distribution is assumed equal to th ambient temperature T_∞ as the first approximation. Then the iterations will be continued until the following condition is satisfied:

$$T^r(X,Y) - T^{r-1}(X,Y) \le 0.0001 \tag{13}$$

Where r represents the number of iteration. The temperature $T(X,Y)$ represents the PCB temperature, and then the following procedure can be followed to predict the module surface temperature (T_{sij}) using the nomenclature of **Fig. 1b**:

$$q_{ij} = q_{1ij} + q_{2ij} + q_{3ij} + q_{4ij} + q_{5ij} + q_{6ij}$$

$$q_{6ij} = q_{ij} - (q_{1ij} + q_{2ij} + q_{3ij} + q_{4ij} + q_{5ij}) \tag{14}$$

$$T_{jun} = q_{6ij} R_{jb} + T(X,Y) \tag{15}$$

$$T_{sij} = -R_{jt} q_{3ij} + T_{jun} \tag{16}$$

where, R_{jt} =junction to top resistance

R_{jb} =junction to board resistance

The value of T_{sij} was initiated at the starting of iteration as:

$$T_{sij}^i = \frac{R_{jt} q_{ij}}{2} + \frac{R_{jb} q_{ij}}{4} + 1.5 T_\infty \tag{17}$$

Then the iteration will be terminated when,

$$T_{sij}^{r} - T_{sij}^{r-1} \leq 0.0001 \quad (18)$$

The values of a_{ij} are found NE (number of electronic components) times, then

$$a_{ij} = \sum_{p=0}^{NE} a_{ij}^{p} \quad (19)$$

The values of convective heat transfer q_{1ij} to q_{5ij} can be found from the relation h_{ij} ($q_{ij} = h_{ij} A_{ij} (T_{ij} - T_{\infty})$). A series of convective and radiative heat transfer coefficients were calculated for each surface using a surface temperature range of ambient (or free stream) to $T_{\infty} + 130^{o} C$ by implementing the empirical equations.

DESIGN OPTIMIZATION: GRADIENT SEARCH

Any function in the vicinity of its minimum can be approximated by a quadratic function by using Taylor series expansion. The quadratic function;

$$F(x) = a + x^{T} b + \frac{1}{2} x^{T} G x \quad (20)$$

Where a is a constant, b is a constant vector and G is a positive definite symmetric matrix which has a minimum at the point x^{*} where x^{*} is given by,

$$\nabla F(x^{*}) = b + G x^{*} = 0$$

i.e. $x^{*} = -G^{-1} b$

From Taylor series;

$$f(x) = f(x_o) + (x - x_o)^{T} \nabla f(x_o) + \frac{1}{2} (x - x_o)^{T} G(x_o)(x - x_o)$$

where;

G is the Hessian matrix $\quad G_{ij} = \dfrac{\partial^2 f}{\partial x_i \partial x_j}$

A reasonable approximation to the minimum for $f(x)$ might be minimum for x. If the latter is at x_m we shall have

$$\nabla f(x_o) + G(x_o)(x_m - x_o) = 0$$

or $x_m = x_o - G^{-1}(x_o) g(x_o)$ (21)

generally $x_{i+1} = x_i - G^{-1}(x_i) g(x_i)$ (22)

or more flexibly, $x_{i+1} = x_i - \lambda_i G^{-1}(x_i) g(x_i)$ (23)

Where λ_i is determined by a search in the direction $G^{-1}(x_i) g(x_i)$.

The Newton-Raphson method is based on this last equation. The gradient search method is based on equations (21) and (23), although it avoids calculating the inverse Hessian matrix $G^{-1}(x_i)$ at each step by setting the search direction at stage i as $-H_i g(x_i)$, where H_i is a positive definite symmetric matrix which is updated at each stage in a manner to make H equal to the inverse Hessian Matrix.

The constraints and the form of the objective function for the optimized meshing can be expressed as the minimum temperature error as the follows:

Min. $z(\Delta x_i, \Delta y_j)$

$$= \sum_{i=1}^{N_x}\sum_{j=1}^{N_y} a_{ij}^{p} \cos(\frac{i^2\pi\Delta x_i^p}{L_1})\cos(\frac{j^2\pi\Delta y_j^p}{L_2}) - \sum_{i=1}^{n}\sum_{j=1}^{m} a_{ij}^{p-1} \cos(\frac{i^2\pi\Delta x_i^{p-1}}{L_1})\cos(\frac{j^2\pi\Delta y_j^{p-1}}{L_2}) \quad (24)$$

From the above we note that the number of design variables ($Nx + Ny$), is a variable also. The constraints are:

$$Nx_L \le Nx \le Nx_U\,,\ \ Ny_L \le Ny \le Ny_U \quad (24a)$$

$$\frac{L_1}{Nx_U} \le \Delta x_i \le \frac{L_1}{Nx_L},\ \frac{L_2}{Ny_U} \le \Delta y_j \le \frac{L_2}{Ny_L},\ \sum_{i=1}^{Nx}\Delta x_i = L_1,\ \sum_{j=1}^{N_y}\Delta y_j = L_2 \quad \textit{(24b)}$$

It will be noted that the numbers of constraints are $m = 6$. Since the number of the design variables ($Nx + Ny$) is variable, we will perform the Complex Method in dual form (new technique or originality point of the present work) as the follows:

1-Construct the external two-dimensional complex of $n = 2$ and $m = 2$ with the same objective function of the internal complex (Eq. (24a)), while the constraints are explicit only.

2-In each iteration step of external complex, the data will be exported to the internal complex of $m = 4$ constraints (Eq. (24b)) and n=($Nx + Ny$) design variables.

3-The optimum mesh of step2 will export to the external complex (step1), and so on until the global optimum is found.

The initial step sizes are:

$$\Delta x_i^i = \frac{L_1}{\left(\frac{Nx_U + Nx_L}{2}\right)} \quad , \quad \Delta y_j^i = \frac{L_2}{\left(\frac{Ny_U + Ny_L}{2}\right)}$$

at the start of iteration we will make;

$$\left.\Delta x_i^{p-1} = \Delta x_i^i, \Delta y_j^{p-1} = \Delta y_j^i\right\}$$

To quantify the maximum permissible heat loss from an electronic module, the heat Q_{loss} can be separated, based on the heat transfer mechanism, into convective heat transfer q_{conv} and radiative heat q_{rad}. The convection heat transfer coefficients for the horizontal PCB are **(Holman. 1989)**:

$$h=\begin{cases} 1.42(\frac{\Delta T}{t})^{0.25} & ,vertical \quad surfaces \\ 1.32\left(\frac{\Delta T}{\frac{2bw}{b+w}}\right)^{0.25} & ,horizontal \quad surfaces \\ 0.61\left(\frac{\Delta T}{\frac{2bw}{b+w}}\right)^{0.2} & ,upset-down \quad surfaces \end{cases} \tag{25}$$

Assuming that the heat transfer through the bottom surface is negligible and that the surface temperature distribution is uniform, the convective heat transfer is given for horizontal PCB (see **Fig. 1b**).

$$Q_{loss}=2\sum_e q_1+2\sum_e q_2+\sum_e q_3+q_{b1}+q_{b2}+q_{rad} \tag{26}$$

Where, $q_1=h_1A_1\Delta T_i=1.42(t_iw_i)(\frac{\Delta T_i}{t_i})^{0.25}\Delta T_i$

$$q_2=h_2A_2\Delta T_i=1.42(b_it_i)(\frac{\Delta T_i}{t_i})^{0.25}=1.42b_it_i^{0.75}\Delta T_i^{1.25}$$

$$q_3=h_3A_3\Delta T_i=1.32(w_ib_i)\left(\frac{\Delta T_i}{\frac{2b_iw_i}{b_i+w_i}}\right)^{0.25}\Delta T_i$$

$$=1.11(b_iw_i)^{0.75}(b_i+w_i)^{0.25}\Delta T_i^{1.25}$$

$$q_{b1}=1.11\left(\frac{L_1+L_2}{L_1L_2}\right)^{0.25}(L_1L_2-\sum_e b_iw_i)(T_b-T_\infty)^{1.25}$$

$$q_{b2}=0.61L_1L_2\left(\frac{\Delta T_1}{\frac{2L_1L_2}{L_1+L_2}}\right)^{0.2}\Delta T_1=0.531(L_1L_2)^{0.8}(L_1+L_2)^{0.2}(T_b-T_\infty)^{1.2}$$

$$q_{rad}=5.669*10^{-8}\left(\sum_e f_e\varepsilon_eA_e(T_{se}^4-T_\infty^4)+(T_b^4-T_\infty^4)(f_{b1}\varepsilon_{b1}A_{b1}+f_{b2}\varepsilon_{b2}A_{b2})\right)$$

Where f_{b1}: Upper surface of PCB radiation shape factor

f_{b2}: Lower surface of PCB radiation shape factor

f_e: Electronic element radiation shape factor

Due to the blockage effect of the desk f_e and f_{b1} is reduced to 0.5 for all surfaces, and bottom surface of element is practically ineffective. Therefore, using typical emissivity values of $\varepsilon_e = 0.9$ for plastic materials, $f_{b2} = 1$ and $\varepsilon_{b1} = \varepsilon_{b2} = 0.7$ is recommended. The above equation can be rewritten as:

$$q_{rad} = 5.669 * 10^{-8} \left(\sum_e \begin{matrix} 0.5\varepsilon_e (b_i w_i + 2b_i t_i + 2w_i t_i)(T_{si}^4 - T_\infty^4) + \{0.5\varepsilon_{b1}(L_1 L_2 - \sum_e w_i b_i) \\ + \varepsilon_{b2} L_1 L_2\}(T_b^4 - T_\infty^4) \end{matrix} \right) \tag{27}$$

The total heat loss can be found by adding **Eq. (26)** to **Eq. (27)** as:

$$\begin{aligned} Q_{loss} &= 2.84(T_{si} - T_\infty)^{1.25} \left\{ \sum_e (b_i + w_i) t_i^{0.75} + 0.3908(b_i + w_i)^{0.25}(b_i w_i)^{0.75} \right\} \\ &+ 1.11(T_b - T_\infty)^{1.25} \left(\frac{L_1 + L_2}{L_1 L_2} \right)^{0.25} (L_1 L_2 - \sum_e b_i w_i) \\ &+ 0.531(T_b - T_\infty)^{1.2} (L_1 L_2)^{0.8} (L_1 + L_2)^{0.2} + q_{rad} \end{aligned} \tag{28}$$

For the vertical PCB, there are two cases. One for the vertical PCB is oriented so as to make L_1 vertical, and the other L_2 is vertical. The first case is as follows:

$$Q_{loss} = \sum_e q_1 + 2\sum_e q_2 + \sum_e q_3 + \sum_e q_5 + q_{b1} + q_{b2} \tag{29}$$

$$q_1 = 0.531(w_i t_i)^{0.8}(w_i + t_i)^{0.2} \Delta T_i^{1.2}, \quad q_2 = 1.42 b_i^{0.75} t_i \Delta T_i^{1.25}$$

$$q_3 = 1.42 b_i^{0.75} w_i \Delta T_i^{1.25}, \quad q_5 = 1.11(w_i t_i)^{0.75}(w_i + t_i)^{0.25} \Delta T_i^{1.25}$$

$$q_{b1} = 1.42(L_1 L_2 - \sum_e w_i b_i) L_1^{-0.25} \Delta T_1^{1.25}, \quad q_{b2} = 1.42 L_1^{0.75} L_2 \Delta T_1^{1.25}$$

For the case of vertical L_2

$$q_{conv.} = 2\sum_e q_1 + \sum_e q_4 + \sum_e q_2 + \sum_e q_3 + q_{b1} + q_{b2} \tag{30}$$

$$q_1 = 1.42 w_i^{0.75} t_i \Delta T_i^{1.25}, \quad q_2 = 0.531(b_i t_i)^{0.8}(b_i + t_i)^{0.2} \Delta T_i^{1.2}$$

$$q_3 = 1.42 w_i^{0.75} b_i \Delta T_i^{1.25}, \quad q_4 = 1.11(b_i t_i)^{0.75}(b_i + t_i)^{0.25} \Delta T_i^{1.25}$$

$$q_{b1} = 1.42(L_1 L_2 - \sum_e b_i w_i) L_2^{-0.25} \Delta T_1^{1.25}, \quad q_{b2} = 1.42 L_1 L_2^{0.75} \Delta T_1^{1.25}$$

OBJECTIVE FUNCTION AND CONSTRAINTS

We can modify the objective function and Constraints in order to be useable in the SUMT method of the present work as follows:

$$z = \Phi(x, r) = f(x) + r \sum_{j=1}^{m} \frac{1}{C_j(x)} \tag{31}$$

1- $f(x)$ equivalent to $\frac{1}{Q_{loss}}$ for Eqs. (28 through 30).

2-The constraints must be in the form

$$C_j(x) \geq 0 \tag{32}$$

Therefore $\underline{b_{iL}} \leq \underline{b} \leq \underline{b_{iU}}$ is equivalent to two constraints as follows:

$$\underline{b} \geq \underline{b_{iL}} \Rightarrow \underline{b} - \underline{b_{iL}} \geq 0 \tag{33}$$

$$\underline{b_{iU}} - \underline{b} \geq 0 \tag{34}$$

In other words, each double inequality constraint can be performed by two inequality constraints of the form $C_j(x) \geq 0$.For example, if we let to optimize Eq. (28), the following form of the objective function will be attained:

$$z = \phi(x, r) = \frac{1}{Q_{loss}} +$$

0 *(35)*

In the case of the optimum heat transfer coefficient h, the empirical relations are not need. In this case, the heat transfer coefficient will be considered as a constraint, which have lower and upper limits ($h_L \leq h \leq h_U$).

RESULTS AND DISCUSSION

The PCB contains a central processing unit CPU dissipating 5W and 12 additional heat dissipating devices, each dissipating 1.5W is considered as a specific example for this paper.

(A) Optimal Local heat Transfer Coefficient

Many cases of PCB thermal design, we need to make the convective heat transfer coefficient optimal for a specified electronic component such as CPU in PC. However, the PCB will be used to optimize convective heat transfer coefficient on each electronic component for the objective function. The constraints for this case are:

$$8 \leq h_i \leq 20 W/m.^o C, 0.76 \leq k_b \leq 13.6 W/m.^o C$$

$$200 \le L_1 \le 500mm,\ 150 \le L_2 \le 400mm$$

$$\frac{b_i}{2} \le CX_i \le L_1 - \frac{b_i}{2},\ \frac{w_i}{2} \le CY_i \le L_2 - \frac{w_i}{2}$$

$$20 \le b_i \le 40mm,\ 60 \le b_{11} \le 90mm,\ 60 \le b_{13} \le 90mm$$

$$4 \le t_i \le 11mm, 20 \le w_i \le 40mm,\ 40 \le w_{11} \le 70mm,\ 50 \le w_{13} \le 70mm$$

$$10 \le Nx \le 100, 10 \le Ny \le 100, T_{jun} \le 130^o C, T_b \ge T_\infty, 4 \le t_s \le 10mm$$

$$CX_i + \frac{b_i}{2} \le L_1, CY_i + \frac{w_i}{2} \le L_2, b_i(T_{si} - T_\infty) \le 5.6$$

$$T_\infty = 25^o C, R_{jt} = 2^o C/W, R_{jb} = 3^o C/W,\ \dot{m} = 0.2kg/s$$

$$L_1^i = 381mm, L_2^i = 263mm, V = 1m/\sec, T_\infty = 25^o C,$$

$$Hum = 0.3, R_{jb=0}, R_{jt} = 0.2^o C/W, k_b = 1.2W/m.^o K$$

$$k_e = 138W/m.^o K, \varepsilon_e = 0.9, \varepsilon_b = 0.5$$

Fig. 2 shows the initial thermal layout. Fig. 3 shows the optimal thermal layout which is being drawn in 1:2 scale. The value of h is indicated on each electronic element. As might be expected from a physical point of view, the first and last columns have a higher heat transfer than the others. This behavior is same as of the forced convection because the flow field is different (impingement and parallel), and causes additional cooling at the front and back, respectively. The values of optimal heat transfer coefficients for components 9, 10, 4, and 2 are converged because they are exposed to the same flow field.

(B) Heat Loss Maximization

For the previous initial inputs and constraints of the optimum thermal layout is shown **Fig. 4**. Three components per column per column represent a good design from the heat loss point of view. For a given circuit board area, the thermal performance will be better if the larger dimension of the board is oriented horizontally rather than vertically. The reason is that there is less"pre-heating" of the air in the horizontal configuration. This can be useful technique to keep in mind, if the system has flexibility with regard to board packaging. From the above results, the components or sub-assemblies with higher power dissipation should be located near the top of the PCB. This will prevent the heated air from these components from raising the ambient temperature of all the circuitry above it. This hot air would result in lower average component temperatures and reliability.

From the previous discussion, we note that the optimal PCB board is vertical in the case of natural convection. In some cases, we need the horizontal or horizontal upset-down orientation to the PCB according to the space limitations. If we not need the global optimum, we will take the optimal results for horizontal and upset down orientation only **Fig. 5** shows the optimum thermal layout for horizontal upset-down PCB orientation. Fig. 6 shows the optimum thermal layout for horizontal PCB orientation. From **Figs. (5)** and **(6)**, we will note the following points:

1- The electronic components of power greater than other components must lie near the edges of the PCB for the case of horizontal orientation. This is due to the overcome the pre-heating from neighboring.

2- Any electronic component that lies near the center of PCB has larger area as compared with other components. This can be taken when the power of this component is small for the horizontal PCB orientation.

3- For the horizontal upset-down PCB orientation, the component of large power must lies near the center. This is because that location gives less preheating to air. Also the thickness of each component t_i is larger than in other PCB orientations. This is because the larger value of t_i will enlarge the side area of the electronic component, which have the same heat transfer coefficient for the vertical flat plate.

4 Thermal conductivity of PCB is a very efficient parameter that controlled to lower the peak temperature in natural convection. Radiation may account as a significant fraction of the total heat loss objective function for the electronic equipment cooling by natural convection.

5 Larger dimension of the PCB must oriented horizontally rather than vertically in free convection for the optimum total heat loss. For the same previous objective function and case of convection, the electronic components or sub-assemblies of larger power should located near the top of the PCB. Also, in the case of the horizontal-Upset-down, the electronic components of larger power must lie near the center of the PCB.

CONCLUDING REMARKS.

1- A new method for optimization of the PCB meshing which is applicable not only for the PCB, but to other system meshing and can be improved to three-dimensional meshing was developed. This method is based on the mathematical optimization (Complex Method). The dual complex method is a new technique to control the PCB meshing and a good route to reach the optimum system mesh i.e. a unique system mesh with minimal CPU time.

2-Larger dimension of the PCB must oriented horizontally rather than vertically in free convection for the optimum total heat loss. For the same previous objective function and case of convection, the electronic components or sub-assemblies of larger power should located near the top of the PCB. Also, in the case of the horizontal-Upset-down, the electronic components of larger power must lie near the center of the PCB.

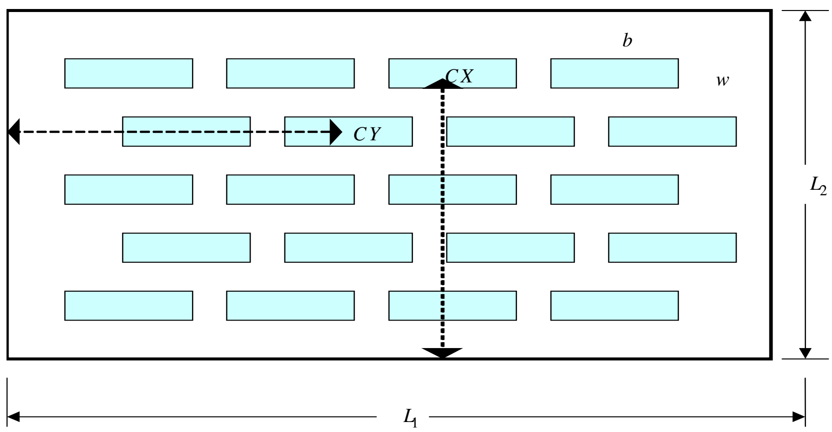

(a)

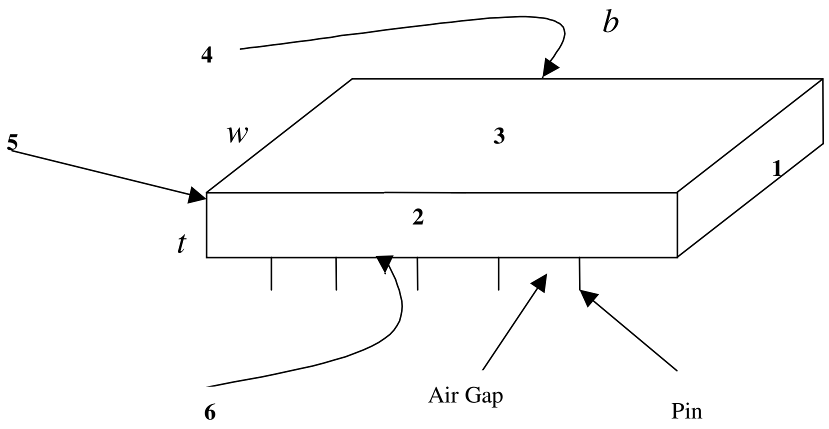

(b)

Fig. 1: Thermal Layout and Heat transfer surfaces.

Horizontal

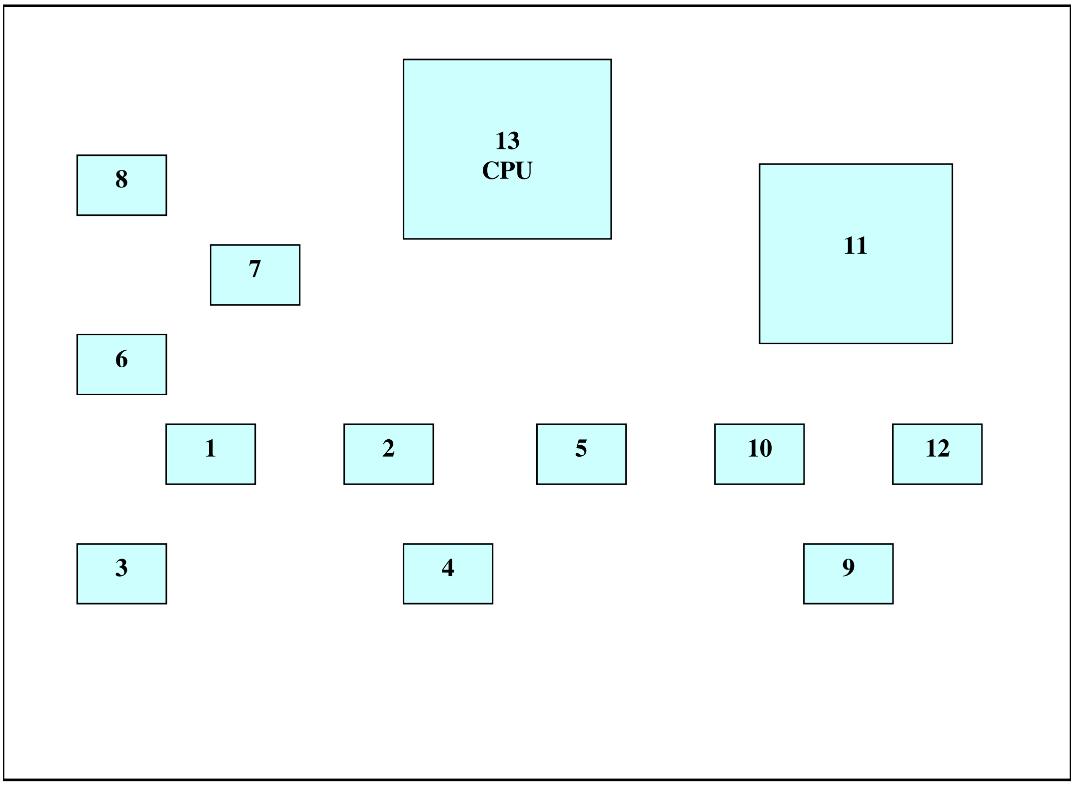

Fig. 2: Initial Thermal Layout of PCB.

Fig. 3: Optimal Thermal Layout for h as an Objective Function.

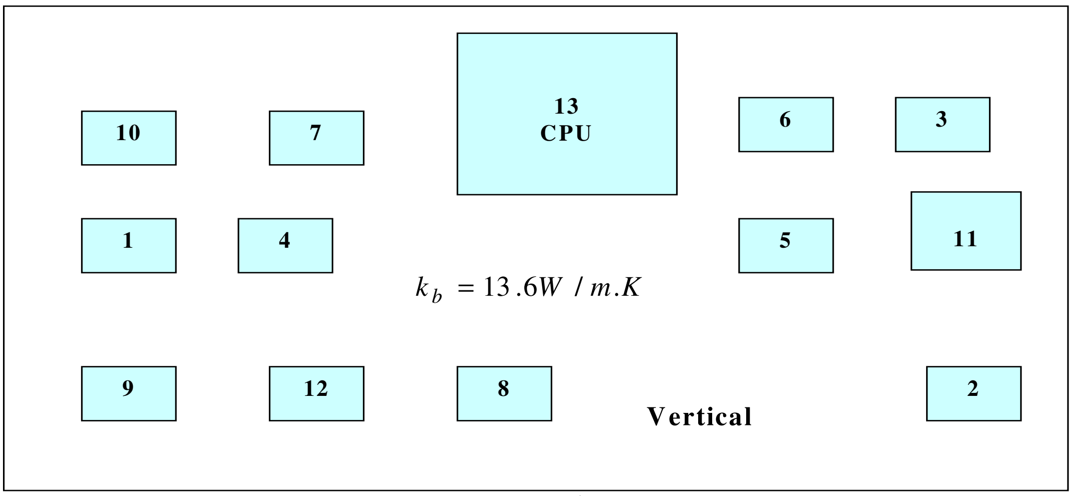

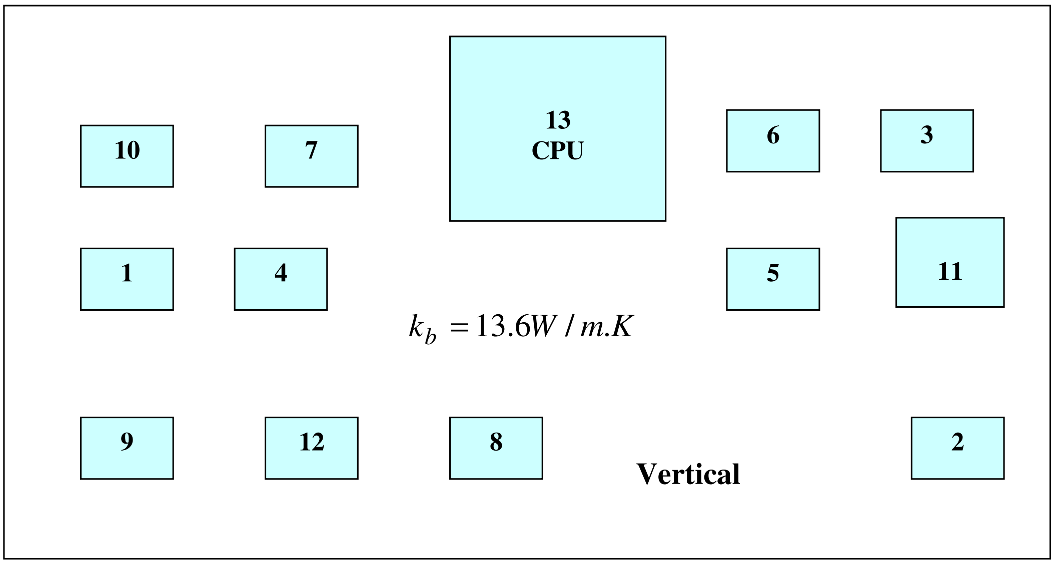

Fig. 4: Optimal Thermal Layout for Q_{loss} Maximization.

Horizontal Upset-Down

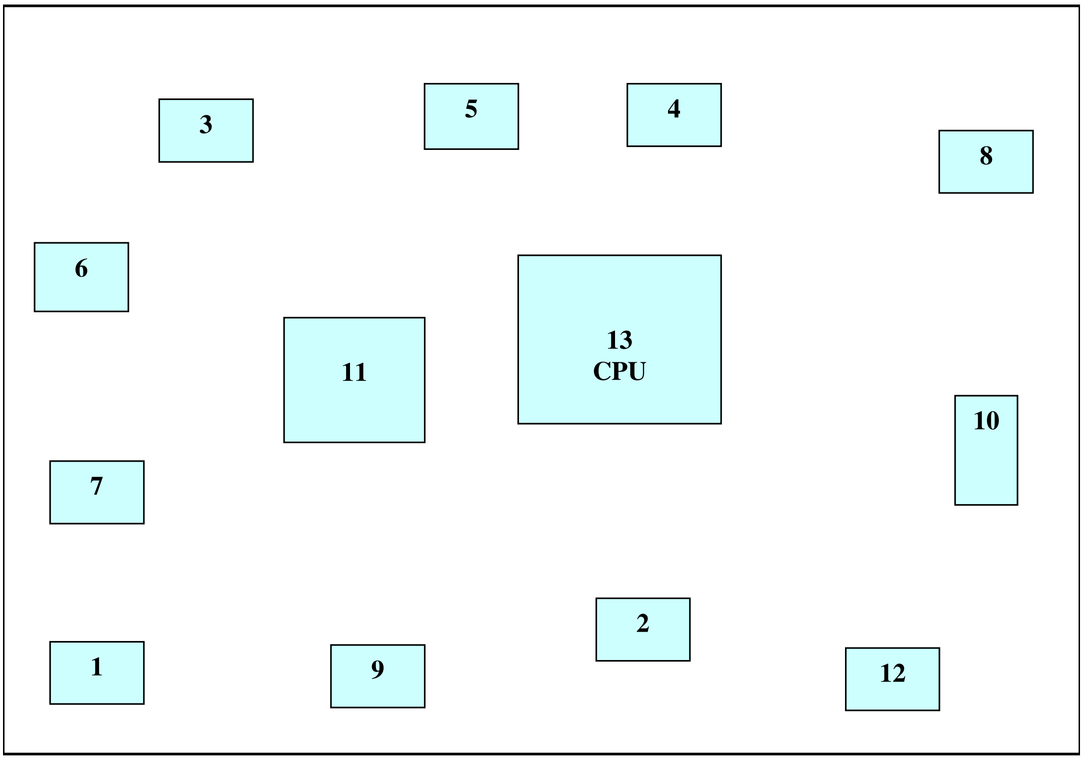

Fig. 5: Optimal Thermal Layout for Max. Q_{loss} for Horizontal Upset-Down Orientation.

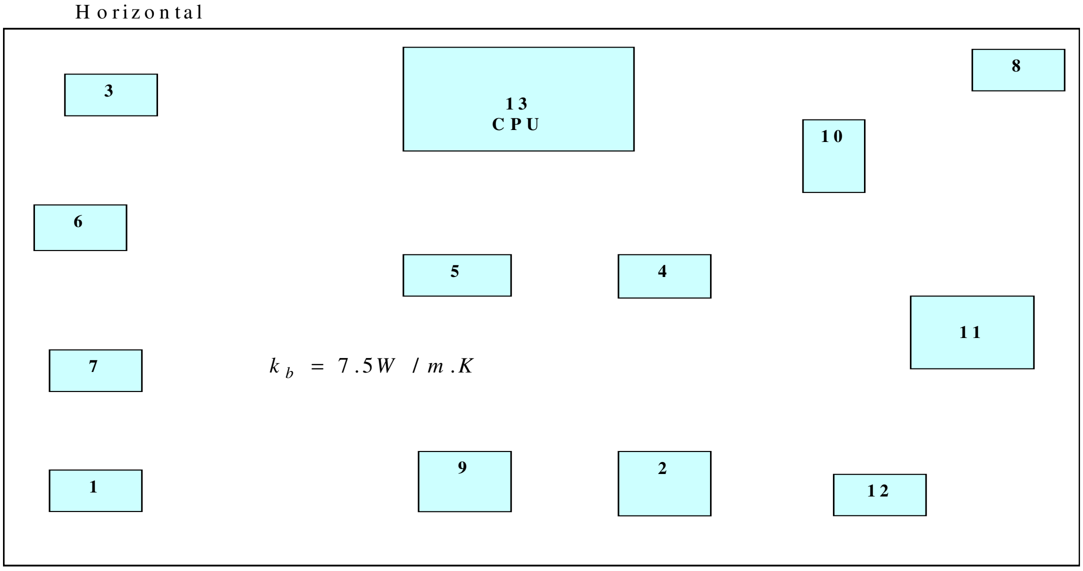

Fig. 6: Optimal Thermal Layout for Max. Q_{loss} for Horizontal PCB Orientation.

REFERENCES

Elias, P. And Sridhar, G., "Natural Convection in Shallow Horizontal Air Layers Encountered in Electronic Cooling" Transaction of the ASME, Vol. 117, DECEMBER, 1995.

Gerlad, R., " Use of Superposition to Describe Heat Transfer from Multiple Electronic Components", Report, July 2, 2001, M.E.D., Portland State University, Portland

Holman, J. P., 1989 ," Heat transfer " 1st ed., McGraw Hill Co., New York.

Lee, S., Culham, J. R., and Yovanovich, M. M., " Conjugate Heat Transfer from a Vertical Plate with Discrete Heat Sources Under Natural Convection ", 1989, Trans. ASME, J. Electronic Packaging, Vol. 111, pp. 261-267.

Lee, S., Culham, J. R., and Yovanovich, M. M., "The Effect of Common Design Parameters on the Thermal Performance of Microelectronic Equipment: Part I-Natural Convection", 1991A, ASME, Heat Transfer in Electronic Equipment, HTD-Vol. 171, pp. 47-54.

Lee, S., Culham, J. R., T. F., and Yovanovich, M. M.," META- A conjugate Heat Transfer Model for Air Cooling of Circuit Boards with arbitrarily located heat sources", 1990, ASME, HTD, Heat Transfer in Electronic Equipment, Vol.171, pp.117-126.

Lee, S., Culham, J. R., and Yovanovich, M. M., "The Effect of Common Design Parameters on the Thermal Performance of Microelectronic Equipment: Part II-Forced Convection", 1991, ASME, Heat Transfer in Electronic Equipment, HTD-Vol. 171, pp. 55-62.

Le Jannou, J.P., Houn, Y., "Representation of Thermal Behavior of Electronic Components for the Creation of a Databank", IEEE transactions on components, hybirds, and manufacturing technology, Vol.14, No.2, pp.366-373, 1991.

Mahaney, H. V., Incropera, F. P., and Ramadyani, S., "Comparison of predicted and measured mixed convection heat transfer from an array of discrete sources in a horizontal rectangular channel", 1990, Int. J. Heat and Mass Transfer, Vol. 33, No. 6, pp.1233-1245.

Ying, F. P., Elaine, P. Scott, and Karen, A. Thole, " Integrated Thermal Design and Optimization Study for Active Integrated Power Electronic Modules(IPEMs)", M. Sc. Thesis, August 26, 2002, Blacksburg, Virginia.

Yovanovich, M.M., Lee, S., and Gayowsky, T.J., 1992, " Approximate Analytic Solution for Laminar Forced Convection from Isothermal Plate,"Paper No.92-0248, AIAA 30th Aerospace Sciences Meeting and Exhibit, Reno, NV, January 6-9.

NOMENCLUTURE

A :*Area,* m^2
b :*Electronic module length,* m
CX,CY:Value of electronic module centers, m
f :*Radiation shape factor*
G :*Hessian Matrix,* $\frac{\partial^2 f}{\partial x_i \partial x_j}$
g: Acceleration of gravity, m/s^2
$g(x)$:*Derivative,* $g(x) = \nabla f(x)$
h :*Heat transfer coefficient,* $W/m^2.^oC$
k_b :*Conduction coefficient for board,* $W/m.^oC$
L_1 :*PCB length,* m
L_2 :*PCB width,* m
m :*Number of constraints*
Ny :*Number of elements in* Y *direction*
n :*Number of design variables*
Nu_x :*Nusselt number,* $\frac{hx}{k}$
Q : *Generated Heat By the Component,* W
q :*Uniform single surface heat flux,* W/m^2
T :*Temperature,* ^oC *or* K
t :*Electronic module height,* m
t_s :*PCB thickness,* m
w :*Electronic module width,* m
x :*Design variable in optimization scheme*
X :*X-direction, horizontal parallel to* L_1
Y :*Y-direction, horizontal parallel to* L_2
z : *Objective function value*

Greek

λ :*Lagrange Multiplier*
ΔT : Temperature difference, ^oC
δ_{gap} :*Air gap thickness,* μm
ε :*Emissivity*
$\Phi(x,r)$:*Unconstraint objective function*